Songklanakarin J. Sci. Technol.
33 (4), 441-448, Jul. - Aug. 2011

SJST SONGKLANAKARIN JOURNAL OF SCIENCE AND TECHNOLOGY
http://www.sjst.psu.ac.th

*Original Article*

# Friction stir welding of dissimilar joint between semi-solid metal 356 and AA 6061-T651 by computerized numerical control machine

Muhamad Tehyo[1]*, Prapas Muangjunburee[2] and Somchai Chuchom[1]

[1] *Department of Industrial Engineering,*

[2] *Department of Mining and Materials Engineering, Faculty of Engineering, Prince of Songkla University, Hat Yai, Songkhla, 90112 Thailand.*

Received 24 January 2010; Accepted 8 August 2011

**Abstract**

The objective of this research is to investigate the effect of welding parameters on the microstructure and mechanical properties of friction stir welded butt joints of dissimilar aluminum alloy sheets between Semi-Solid Metal (SSM) 356 and AA 6061-T651 by a Computerized Numerical Control (CNC) machine. The base materials of SSM 356 and AA 6061-T651 were located on the advancing side (AS) and on the retreating side (RS), respectively. Friction Stir Welding (FSW) parameters such as tool pin profile, tool rotation speed, welding speed, and tool axial force influenced the mechanical properties of the FS welded joints significantly. For this experiment, the FS welded materials were joined under two different tool rotation speeds (1,750 and 2,000 rpm) and six welding speeds (20, 50, 80, 120, 160, and 200 mm/min), which are the two prime joining parameters in FSW. A cylindrical pin was adopted as the welding tip as its geometry had been proven to yield better weld strengths. From the investigation, the higher tool rotation speed affected the weaker material's (SSM) maximum tensile strength less than that under the lower rotation speed. As for welding speed associated with various tool rotation speeds, an increase in the welding speed affected lesser the base material's tensile strength up to an optimum value; after which its effect increased. Tensile elongation was generally greater at greater tool rotation speed. An averaged maximum tensile strength of 197.1 MPa was derived for a welded specimen produced at the tool rotation speed of 2,000 rpm associated with the welding speed of 80 mm/min. In the weld nugget, higher hardness was observed in the stir zone and the thermo-mechanically affected zone than that in the heat affected zone. Away from the weld nugget, hardness levels increased back to the levels of the base materials. The microstructures of the welding zone in the FS welded dissimilar joint can be characterized both by the re-crystallization of SSM 356 grains and AA 6061-T651 grain layers.

**Keywords:** SSM 356, AA 6061-T651, Friction stir welding (FSW), dissimilar joint, CNC

## 1. Introduction

In recent years, demands for light-weight and/or high-strength sheet metals such as aluminum alloys have steadily increased in aerospace, aircraft, and automotive applications because of their excellent strength to weight ratio, good ductility, corrosion resistance and cracking resistance in adverse environments. Semi-Solid Metals (SSM), mostly aluminum alloys, have emerged in the usage of casting components in various applications. Joining between SSM 356 casting aluminum alloy and AA 6061-T651 is a common combination that requires good strength joints and an easy process. Joining of aluminum alloys has been carried out with a variety of fusion and solid state welding processes. Friction stir welding (FSW) was a process invented by Wayne Thomas at the Welding Institute (TWI) and the patent appli-

* Corresponding author.
Email address: tehyo_m@hotmail.com

cation was first filed in the United Kingdom in December 1991 (Thomas *et al*., 1991). FSW as a solid-state joining technology process is one of the environmental friendly processes using frictional heat generated by rotation and traversing of tool with a profiled pin along the butt weld joint. Figure 1. illustrates the schematic drawing of the FSW process. When frictional heat is generated materials get softened locally and plastic deformations of the work pieces occur. Tool rotation and translation expedite material flow from front to back of the pin and a welded joint is produced (Liu *et al*., 1997). This method has attracted a great amount of interests in a variety of industrial applications in aerospace, marine, automotive, construction, and many others of commercial importance (Lohwasser, 2000). FSW can produce a high-quality joint compared to other conventional welding processes, and also makes it possible to join nonmetals and metals, which have been considered as non-weldable by conventional methods (Su *et al*., 2003). The advantages of the solid-state FSW process also encompass better mechanical properties, low residual stress and deformation, weight savings, and reduced occurrence of defects (Salem *et al*., 2002).

FSW had been carried out between conventional cast A356 and 6061-T6 aluminum alloys (Lee *et al*., 2003). They had observed that, the weld zone microstructure is dominated by the retreating side substrate. The hardness distribution was governed by precipitation of the second phase, distribution of Si particles and dislocation density. Maximum bond strength of the transition joint was close to A356 Al alloy.

Observations of FSW of dissimilar metals, namely 6061 aluminum to copper have illustrated complex flow phenomena as a consequence of differential etching of the intercalated phases producing high contrast and even high resolution flow patterns characteristic of complex (intercalation) vortices, swirls, and whorls (Murr *et al*., 1998). However, welds in this Al:Cu systems are difficult to achieve and there is usually a large void tunnel near the weld base. There have been numerous and revealing microstructural observations in the dissimilar Al:Cu system, but systematic studies for more efficient welds should be made in other dissimilar aluminum alloy systems where differential etching can produce sufficiently high contrast to allow for flow visualization.

In this work, dissimilar joints between the recently invented SSM 356 aluminum alloy, which is produced by a gas induced semi-solid (GISS) process (Wannasin *et al*., 2006) and conventional AA 6061-T651 were studied. SSM 356 aluminum alloy was deployed to replace the use of conventional cast A356 in this study so as to eliminate and/or lessen drawback properties associated with it. Welding parameters, particularly the tool rotation speeds and the welding speed, and joint properties were the main characteristics in the investigation.

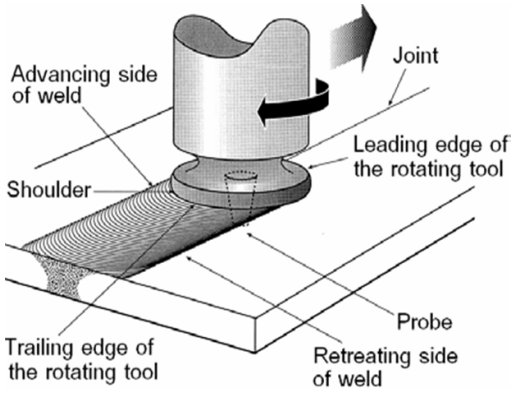


Figure 1. Schematic drawing of friction stir welding (FSW).

## 2. Experimental

### 2.1 Materials

The base materials used for FSW in the present study were 4 mm. thick plates of aluminum cast SSM 356 and wrought aluminum alloy AA 6061-T651. Their chemical compositions and mechanical properties are listed in Table 1. The microstructure of the base materials are shown in Figure 2. SSM 356 exhibited a typical globular grain structure while AA 6061-T651 revealed an equiaxed structure with many etch-pits, which may be sites of second precipitate particles. The plates were cut and machined into rectangular welding specimens of 100 mm × 50 mm cross-section. A schematic diagram of FSW with sampling location is shown in Figure 3. SSM 356 was fixed at the advancing side and AA 6061-T651 was laid on the retreating side. Both SSM 356 and AA6061-T651 were rigidly clamped in order to minimize vibration and/or displacement during processing.

Table 1. Chemical compositions (% weight) and mechanical properties of the base materials.

| Materials | Si | Fe | Cu | Mn | Mg | Zn | Ti | Cr | Ni | Al |
|---|---|---|---|---|---|---|---|---|---|---|
| SSM 356 | 7.74 | 0.57 | 0.05 | 0.06 | 0.32 | 0.01 | 0.05 | 0.02 | 0.01 | Bal. |
| AA 6061-T651 | 0.60 | 0.70 | 0.28 | 0.15 | 1.00 | 0.25 | 0.15 | 0.20 | - | Bal. |

| Properties | Ultimate tensile strength (MPa) | Yield strength (MPa) | Elongation (%) |
|---|---|---|---|
| SSM 356 | 198 | 131 | 9.7 |
| AA 6061-T651 | 290 | 240 | 10.2 |

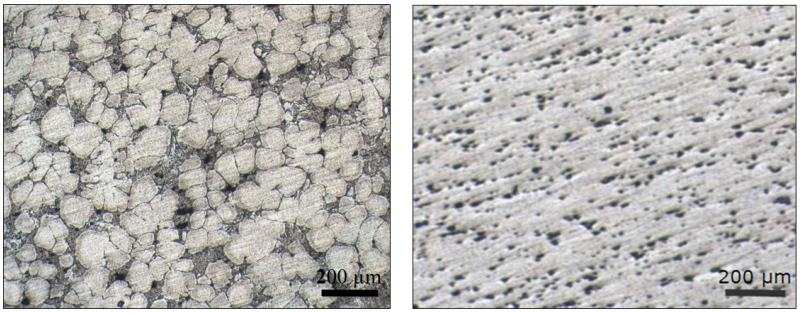


Figure 2. Microstructures of the base materials: (left) SSM 356, (right) AA 6061-T651.

### 2.2 Welding tool size and welding parameters

A non-consumable tool made of JIS-SKH 57 tool steel was used to fabricate the joints. The cylindrical pin used as the welding tool is shown in Figure 4. The tool has a shoulder diameter, pin diameter and pin length of 20 mm, 5 mm and 3.6 mm, respectively. The stationary welding tool rotates in clockwise direction, while the specimens, tightly clamped in position to the backing plate on the CNC machine table, travelled forward. In general, tool setting, the tool pin tilts at a degree to the vertical, while the machine bed is horizontal. In the CNC welding machine, however, the vertical tool pin cannot be tilted and hence an adaptation was designed and attached to the horizontal machine bed to create the required tilt angle. In this study, tool parameters were fixed at 4.4 kN of downward tool plunge force and 3 degree tool tilt angle (Figure 5). The direction of welding was normal to the rolling direction. Single pass welding procedure was adopted to fabricate the joints. Welding parameters investigated were tool rotation speed and welding speed. The values of these parameters are listed in Table 2. Three joints at two different tool rotation speed levels and six welding speeds made up a total of 36 joints (3×2×6) fabricated in this investigation.

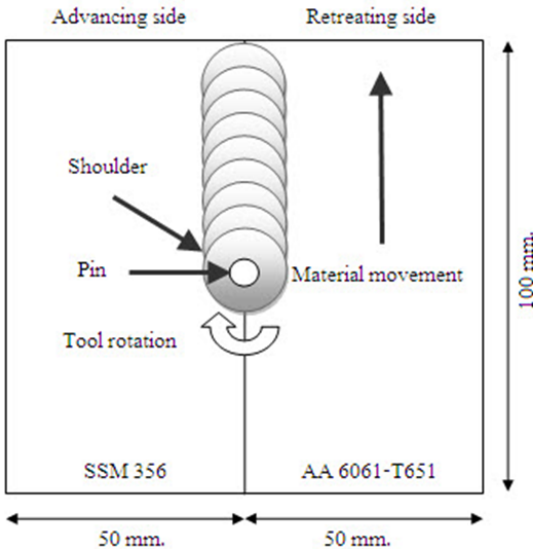


Figure 3. Schematic diagram illustrating the FSW processing. The retreating side is anti-parallel in relation to the tool rotation direction and the plate travel direction.

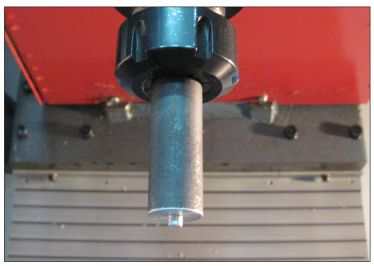

Figure 4. Illustration of the tool used in the present study.

### 2.3 NC program

In this experiment, the tool path and the NC program for the Cincinnati A2100 FSW CNC machine are shown in Figure 5. and Table 3.

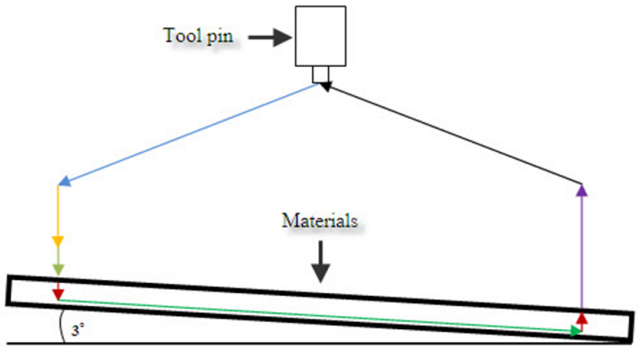


Figure 5. Schematic illustration of the tool path for this experiment.

Table 2. Welding parameters and variables.

| Welding parameters | |
|---|---|
| *Tool rotation speed, rpm* | *Welding speed, mm/min* |
| 1,750, 2,000 | 20, 50, 80, 120, 160, 200 |

Table 3. NC program for FSW of dissimilar joint.

| No. | Command | Description |
|---|---|---|
| N0010 | : G90 G94 G17 G71 G40 | Absolute positioning mode, Metric unit |
| N0020 | T18 M06 | Tool change number 18 |
| N0030 | S** M03 | Spindle speed on clockwise ** rpm |
| N0040 | G01 X0 Y0 Z100 F1,500 | Linear interpolation feed rate 1,500 mm/min |
| N0050 | G01 Z10 F1,000 | Linear interpolation feed rate 1,000 mm/min |
| N0060 | G01 Z0 F100 | Linear interpolation feed rate 100 mm/min |
| N0070 | G01 Z-3.73 F6 | Linear interpolation feed rate 6 mm/min |
| N0080 | G04 F55 | Dwell time is 55 sec. |
| N0090 | G01 Z-7.92 Y-79.89 F* | Linear interpolation feed rate * mm/min |
| N0100 | G04 F10 | Dwell time is 10 sec. |
| N0110 | G01 Z-4 F12 | Linear interpolation feed rate 12 mm/min |
| N0120 | G01 Z10 F1,000 | Linear interpolation feed rate 1,000 mm/min |
| N0130 | G01 Y0 Z100 F1,500 | Linear interpolation feed rate 1,500 mm/min |
| N0140 | M05 | Spindle turned off |
| N0150 | M30 | End of program |

**Note:** ** ; Tool rotation speed (rpm), * ; Welding speed (mm/min)

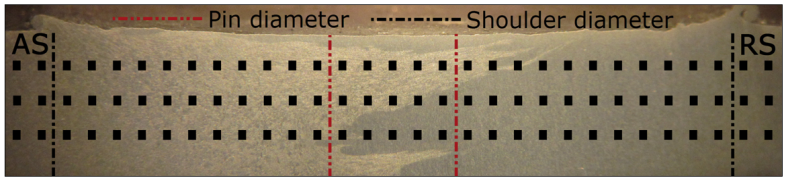


Figure 6. Microhardness test position profiles.

### 2.4 Macro and micrographic

For the analysis of microstructural changes due to the FSW process, the joints were cross-sectioned perpendicularly to the welding direction and etched with Keller's reagent. Microstructures were acquired at different zones: transition between welded and base material, welded material, and base material. Following FSW, sections were cut from the weld zone to expose the flow pattern geometries. These sections were polished and etched using Keller's reagent. The SSM 356 aluminum alloy was usually most responsive to this etch and the etching difference between the SSM 356 aluminum alloy and AA 6061-T651 aluminum alloy components could be adjusted by slight variations in composition, exposure or etching time, and temperature to produce high contrast images. Significant variations in the Keller's reagent component concentration could shift the etching preference to the AA 6061-T651 aluminum alloy as well. In this way the flow patterns could be visualized by metallographic contrast in light microscopy.

### 2.5 Hardness and tensile strength

The Vickers hardness across the weld nugget (WN), thermo-mechanically affected zone (TMAZ), heat affected zone (HAZ), and the base materials was measured on a cross-section perpendicular to the welding direction using Vicker's microhardness tester HWDM-3 Type A at a load of 100 gf on the diamond indenter for 10 s. The hardness profiles (Figure 6.) were obtained at the top, middle, and bottom portions of the cross-section and into the base materials of the sample and the average means were reported. The sub-size tensile test specimens with gage length 25 mm, width 6 mm, total length 100 mm and fillet radius of 6 mm were machined (Figure 7.) and tested according to American Society for Testing and Materials (ASTM E8M) standard on an initial strain rate of $1.67\times10^{-2}$ mm/s at room temperature. The tensile properties of the joint were evaluated using three tensile specimens in each condition prepared from the same joint. All specimens

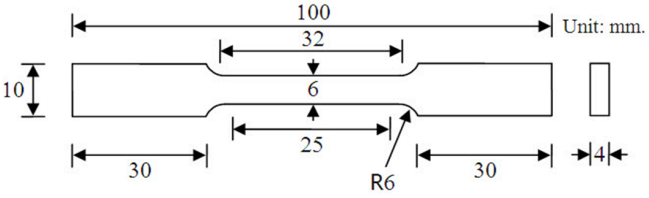


Figure 7. Dimensions of the tensile specimen according to ASTM E8M.

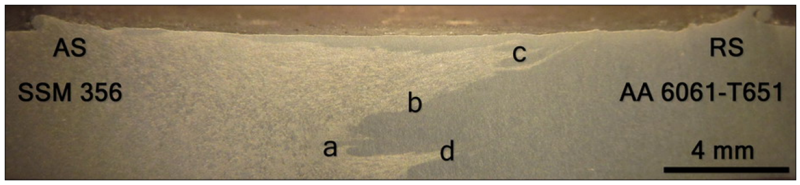


Figure 8. Macrographic of FSW of the dissimilar joint.

were mechanically polished before tests in order to eliminate the effect of possible surface irregularities.

## 3. Results and Discussion

### 3.1 Macro and micrographic

Figure 8 shows a macrographic overview of the cross-section of the dissimilar friction stir welded joints of SSM 356 and AA 6061-T651, at the optimal condition for this experiment (tool rotation speed 2,000 rpm and welding speed 80 mm/min). Since these two aluminum alloys have different etching responses, material flows from the two sides were clearly visible in the weld nugget (WN), which appeared to be composed of different regions of both the alloys which were severely plastically deformed. It can be seen that both materials are sufficiently stirred in the weld zone, where AA 6061-T651 on the RS moves to the AS near the upper surface, while SSM 356 on the AS moves to the RS near the lower surface. The stir zone reveals a mixture of fine recrystallized grains of SSM 356 and AA 6061-T651 and a double basin-shaped appearance with a zigzagged boundary between the two alloys. Combined influence of temperature and plastic deformation induced by the stirring action causes the re-crystallized structure. In all FSW literatures on aluminum alloys, the initial elongated grains of the base materials are converted to a new equiaxed fine grain structure. This experiment confirms the behavior. The grain structure within the nugget is fine and equiaxed and the grain size is significantly smaller than that in the base materials due to the higher temperature and extensive plastic deformation by the stirring action of the tool pin. During FSW, the tool acts as a stirrer extruding the material along the welding direction. The varying rate of the dynamic recovery or recrystallization is strongly dependent on the temperature and the strain rate reached during deformation.

The welding process created a zone affected by the heat generated during the welding. The grain structure within the thermo-mechanically affected zone (TMAZ) is evident from optical microscopy observation. The structure is elongated and exhibits considerable distortions due to the mechanical action from the welding tool. Microstructural details of the dissimilar joint are presented in Figure 9. In Figure 9(a). the interface between the friction stir processes (FSP) is relatively sharp on the AS. In Figure 9(b). the boundary line between SSM 356 (top) and AA 6061-T651 (bottom) is distinctly visible, indicating that FSW is a solid state process. In Figure 9(c). striations formed due to the tool rotation can be seen. In Figure 9(d). different zones in the mixture of the two alloys at the tool's pin edge are clearly visible.

### 3.2 Hardness

Microhardness distribution data on the transverse cross-section of joints welded at all welding conditions are summarized in Figure 10. Softening is noted throughout the weld zone in the SSM 356 and AA 6061-T651 and its average value increased with welding speed. The softening of hardness can probably be attributed mainly to the coarsening and dissolution of strengthening precipitates induced by the thermal cycle of the FSW. Higher hardness was observed in the WN center more than in the TMAZ and HAZ. However, hardness in the SZ and TMAZ regions were slightly lower in comparison with that of the base materials. The final leg of the W-shaped profile was visualized as the microhardness values increased with increasing distance from the weld centerline until base material microhardness values were reached. Away from the weld nugget, hardness levels increase up to the levels of the base materials.

### 3.3 Tensile strength of joints

Tensile properties and fracture locations of joints welded at different welding conditions are summarized in

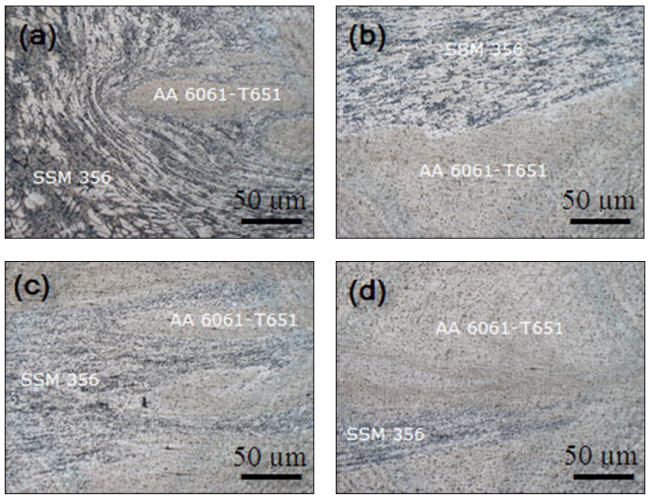


Figure 9. Micrographics of FSW of the dissimilar joint.

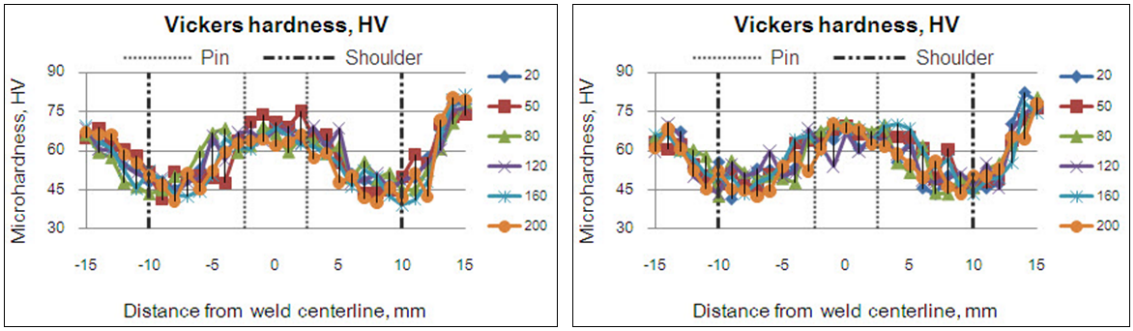


Figure 10. Microhardness profiles across the weld region at tool rotation speed 1,750 rpm (left), and 2,000 rpm (right).

Table 4. Mechanical properties and fracture locations of the welded joints in transverse direction to the weld centerline.

| Tool rotation speed (rpm) | Welding speed (mm/min) | Tensile properties at room temperature | | |
|---|---|---|---|---|
| | | Tensile strength (MPa) | Elongation (%) | Fracture location |
| 1,750 | 20 | 187.1 | 7.291 | SZ |
| | 50 | 192.6 | 8.736 | HAZ of SSM 356 |
| | 80 | 190.4 | 8.206 | TMAZ of SSM 356 |
| | 120 | 191.7 | 7.926 | TMAZ of AA 6061 |
| | 160 | 186.1 | 6.941 | SZ |
| | 200 | 180.3 | 7.208 | SZ |
| 2,000 | 20 | 190.2 | 8.682 | TMAZ of SSM 356 |
| | 50 | 193.4 | 9.316 | TMAZ of SSM 356 |
| | 80 | 197.1 | 8.451 | HAZ of SSM 356 |
| | 120 | 195.7 | 7.796 | TMAZ of SSM 356 |
| | 160 | 195.8 | 8.109 | TMAZ of AA 6061 |
| | 200 | 191.3 | 7.663 | SZ |

Table 4. From the investigation, the higher tool rotation speed leads to a higher tensile strength. A maximum average tensile strength value of 197.1 MPa was attained for a joint produced at the tool rotation speed of 2,000 rpm and the welding speed of 80 mm/min. Tensile properties of FSW butt joints of SSM 356 plate and AA 6061-T651 plate depends mainly on welding defects and hardness of the joint. Fractures occurred at the TMAZ and HAZ of SSM 356 in case of defect-free joints. However, fractures occurred in the SZ for joints consisting of defects.

Equation (1) (Kim *et al.*, 2006) outlines the relationships between heat input, pressure, tool rotation speed, welding speed and other factors. In tool rotation speed versus tensile strength of the welded joints, at the lower tool rotation speed (1,750 rpm) frictional heat generated was less, resulting in poor plastic flow of the materials being welded and thus lower tensile strengths were observed, at higher tool rotation speed (2,000 rpm) metallurgical transformation such as solubilisation, re-precipitation, coarsening and strengthening precipitated in the weld zone, lowering the dislocation density (Threadgill, 1997, Benavides *et al.*, 1999, Lomolino *et al.*, 2005) and increased the tensile strength of the welded joints. Variation in tensile strengths at different tool rotation speed was due to different material flow behavior and frictional heat generated. The maximum tensile strength of the dissimilar FS welded joint was obtained under a welding speed of 50 mm/min for the tool rotation speed of 1,750 rpm, and a welding speed of 80 mm/min for the tool rotation speed of 2,000 rpm.

$$Q = \frac{4\pi^2 \alpha \mu P N R^3}{3V} \quad (1)$$

where Q is the heat input per unit length (J/mm), $\alpha$ is the heat input efficiency, $\mu$ is the friction coefficient, P is the pressure (N), N is the tool rotation speed (rpm), R is the radius of the shoulder (mm), and V is the welding speed (mm/min).

An increase in the welding speed affected lesser the tensile strength of the specimen up to a certain speed. However, further increase in the welding speed beyond that resulted in a decrease in the tensile strength of the weld. At the lowest welding speed (20 mm/min), as well as the highest

welding speed (200 mm/min), lower tensile strengths were observed. The lowest welding speed generated high heat input and encouraged metallurgical transformations of the weld zone leading to a lower tensile strength. The highest welding speed discouraged clustering effect of strengthening precipitates, plastic flow of materials (Flores *et al*., 1998; Murr *et al*., 1998; Sato, 2003; Su *et al*., 2003; Srivatsan *et al*., 2007) and localization of strain (Srivatsan *et al*., 2007) due to insufficient frictional heat generated (Colligan *et al*., 2003; Shanmuga *et al*., 2010).

## 4. Conclusion

In the present study, SSM 356 and AA 6061-T651 aluminum alloys joined by FSW under two different tool rotation speeds and six welding speeds were investigated. Summarizing the main features of the results, following conclusions can be drawn:

1. The microstructures of dissimilar-formed SSM 356 and AA 6061-T651 joints revealed that recrystallized mixed structure of two materials can be easily identified by etching responses of both materials in the stir zone.

2. Hardness observed in the weld center was higher than that in the TMAZ and HAZ. However, hardness in all regions was less comparing with the base materials. The final leg of the W-shaped vickers hardness profile on the cross section increased with increasing distance from the weld centerline to the value of the base materials.

3. In this study, a higher tool rotation speed of 2,000 rpm resulted in a higher tensile strength of the FS welded specimen. A maximum average tensile strength value of 197.1 MPa was recorded for a joint fabricated at the tool rotation speed of 2,000 rpm and at a welding speed of 80 mm/min.

4. An increase in the welding speed appeared to lead to an increase in the tensile strength of the specimen. In fact, the tensile strength approached a maximum value close to the lesser of the parent base materials then decreased with increasing welding speed on the dissimilar FS welded specimens. Thus, neither a too low welding speed (below 80 mm/min) nor a too high welding speed (beyond 80 mm/min) is desirable.

## Acknowledgments

This work was supported by a research fund from the Graduate School, Prince of Songkla University.

## References

Benavides, S., Li, Y., Murr, L.E., Brown, D. and McClure, J.C. 1999. Low temperature Friction Stir welding of 2024 aluminum. Scripta Materialia. 41(8), 809-815.

Colligan, J., Paul, J., Konkol, James, J., Fisher, Pickens Joseph, R. 2003. Friction stir welding demonstrated for combat vehicle construction. Welding Journal. 1-6.

Flores, O.V., Kennedy, C., Murr, L.E., Brown, D., Pappu, S., Nowak, B.M. 1998. Microstructural issues in a friction-stir-welded aluminum alloy. Scripta Materialia. 38(5), 703-708.

Kim, Y.G., Fujii, H., Tsumura, T., Komazaki, T. and Nahata, K. 2006. Three defect types in friction stir welding of aluminum die casting alloy. Materials Science and Engineering A. 415, 250-254.

Lee, W.B., Yeon, Y.M. and Jung, S.B. 2003. The joint properties of dissimilar formed Al alloys by friction stir welding according to the fixed location of materials. Scripta Metallurgica. 49, 423-428.

Liu, G., Murr, L.E., Niou, C., McClure, J.C., and Vega, F.R. 1997. Microstructural Aspects of the Friction Stir Welding of 6061-T6 Aluminum. Scripta Metallurgica. 37, 355-361.

Lohwasser, D. 2000. Proceedings of the 2nd International Symposium on Friction Stir Welding, Gothenburg, Sweden.

Lomolino, S., Tovo, R. and Dos Santos, J. 2005. On the fatigue behavior and design curves of friction stir butt welded Al alloys. International Journal of Fatigue. 27, 305-316.

Murr, L.E., Ying Li., Flores, R.D., Elizabeth, A., Trillo and McClure, J.C. 1998. Intercalation vortices and related microstructural features in the friction stir welding of dissimilar metals. Materials Research Innovations Journal. 2, 150.

Murr, L.E., Liu, G., Mc Clure, J.C. 1998. A TEM study of precipitation and related microstructures in friction-stir-welded 6061 aluminum. Journal of Materials Science and Engineering. 33(5), 1243-1251.

Salem, H.G., Reynolds, A.P. and Lyons, J.S. 2002. Microstructure and retention of superplasticity of friction stir welded superplastic 2095 sheet. Scripta Materialia. 46, 337-342.

Sato, Y.S., Urata, M., Kokawa, H., Ikeda, K. 2003. Hall-petch relationship in friction stir welds of equal channel angular-pressed aluminium alloys. Materials Science and Engineering A. 354, 298-305.

Shanmuga Sundaram, N. and Murugan, N. 2010. Tensile behavior of dissimilar friction stir welded joints of aluminium alloys. Materials and Design. 31, 4184-4193.

Srivatsan, T.S., Satish Vasudevan. and Lisa Park. 2007. The tensile deformation and fracture behavior of friction stir welded aluminum alloy 2024. Materials Science and Engineering A. 466, 235-245.

Su, J.Q., Nelson, T.W., Mishra, R. and Mahoney, M. 2003. Microstructural investigation friction stir welded 7050-T651 aluminum. Acta Materialia. 51, 713-729.

Threadgill, P. 1997. Friction stir welds in aluminum alloys preliminary microstructural assessment, TWI Bulletin - The Welding Institute, Abington, United Kingdom; Industrial Report No: 513/2/97.

Thomas, W.M., Nicholas, E.D., Needham, J.C., Murch, M.G., Templesmith, P. and Dawes, C.J. 1991. Friction Stir Welding, International Patent Application No. PCT/GB 92102203 and Great Britain Patent Application No. 9125978.8.

Wannasin, J., Martinez, R.A. and Flemings, M.C. 2006. A Novel Technique to Produce Metal Slurries for Semi-Solid Metal Processing. Solid State Phenomena. 116-117, 366-369.